KSÜ Mühendislik Bilimleri Dergisi, 28(2), 2025
Araştırma Makalesi

KSU J Eng Sci, 28(2), 2025
Research Article

Kahramanmaras Sutcu Imam University
Journal of Engineering Sciences

Geliş Tarihi : 10.01.2025
Kabul Tarihi : 22.01.2025

Received Date : 10.01.2025
Accepted Date : 22.01.2025

HAVA GÖRÜNTÜLERİNİN DERİN ÖĞRENMESİ KULLANILARAK DAĞINIK FOTOVOLTAİK PİLLERİN OTOMATİK HARİTALANMASI VE SEGMENTASYONU

AUTOMATIC MAPPING AND SEGMENTATION OF SCATTERED PHOTOVOLTAIC BATTERIES USING DEEP LEARNING OF AERIAL IMAGERY

Sinan ALTUN[1] (ORCID: 0000-0002-2356-0460)

[1] Kahramanmaraş İstiklal İmam Üniversitesi, Yapı İşleri ve Teknik Daire Başkanlığı, Kahramanmaraş, Türkiye

*Sorumlu Yazar / Corresponding Author: Sinan ALTUN, s.altun@yaani.com

ÖZET

Güneş enerjisi sistemleri arasında fotovoltaik piller aracılığıyla elektrik enerjisi üretimi, dünya genelinde yaygın bir eğilim haline gelmiştir. Güneş enerjisinin sınırsız bir kaynak olarak değerlendirilmesi ve geleneksel enerji santrallerinin yüksek sera gazı emisyonlarının fotovoltaik pillerle elektrik üretiminde bir engel teşkil etmemesi, küresel ısınmanın tehdit oluşturduğu günümüzde bu yöntemi oldukça cazip kılmaktadır. Bu çalışmada, Türkiye'nin önde gelen üç metropolü olan İstanbul, Ankara ve İzmir'deki dağıtık fotovoltaik sistemler, hava görüntüleri aracılığıyla incelenmiştir. İnceleme süreci, derin öğrenme teknikleri kullanılarak gerçekleştirilmiştir. Bilgilerimize göre, Türkiye'de bu alanda gerçekleştirilen ilk araştırmadır. Ülkede fotovoltaik sistemlere dair hava görüntülerini içeren bir veri seti bulunmadığı için, test veri setinin oluşturulmasında Google Earth platformu kullanılmıştır. Çalışmanın amacı, dünya genelinde ilgi gören hava fotoğraflarını kullanarak Türkiye'de güneş enerjisi sistemleri pazarının büyüme potansiyelini araştırmaktır. Elde edilen sınıflandırma ve segmentasyon sonuçları başarılı olup, dünya genelindeki benzer hava görüntüleri ile Türkiye için güneş enerjisi sistemleri pazar analizi yapılabileceğini ortaya koymaktadır. Sınıflandırma skorları: AlexNet AUC skoru 0.9, GoogLeNet 0.87 ve Inception için 0.83

Anahtar Kelimeler: Fotovoltaik, hava görüntüleri, derin öğrenme, görüntü segmentasyonu

ABSTRACT

Among solar energy systems, the generation of electrical energy through photovoltaic cells has become a widespread trend worldwide. The fact that solar energy is considered as an unlimited resource and the high greenhouse gas emissions of conventional power plants do not constitute an obstacle in electricity generation with photovoltaic cells makes this method very attractive today, when global warming is a threat. In this study, distributed photovoltaic systems in three leading metropolises of Turkey, Istanbul, Ankara, and Izmir, are analysed through aerial imagery. The investigation process was carried out using deep learning techniques. To the best of our knowledge, this is the first research in this field in Turkey. Since there is no dataset containing aerial images of photovoltaic systems in the country, Google Earth platform was used to create the test dataset. The aim of the study is to investigate the growth potential of the solar energy systems market in Turkey by using aerial photographs, which have attracted worldwide attention. The classification and segmentation results obtained are successful and reveal that solar energy systems market analysis can be made for Turkey with similar aerial images around the world. Classification scores: AUC value is 0.9 for AlexNet, 0.87 for GoogLeNet, and 0.83 for Inception.

Keywords: Photovoltaic, Aerial imagery, Deep learning, Image segmentation

ToCite: ALTUN, S., (2025). AUTOMATİC MAPPİNG AND SEGMENTATİON OF SCATTERED PHOTOVOLTAİC BATTERİES USİNG DEEP LEARNİNG OF AERİAL IMAGERY. *Kahramanmaraş Sütçü İmam Üniversitesi Mühendislik Bilimleri Dergisi*, 28(2), 835-850.

INTRODUCTION

Human society is progressively harnessing solar radiation for energy production. In 2020, global electricity consumption for building heating reached 260,300 TWh, representing approximately 50% of total final energy usage; of this, solar thermal (ST) applications contributed 407 TWh (Weiss & Spörk, 2021). Notably, the global photovoltaic (PV) market is currently expanding at a rate that surpasses that of the ST market (IEA PVPS task 1 et al., 2021) and has consistently outperformed expectations over the past decade (Jaxa-Rozen & Trutnevyte, 2021; Victoria et al., 2021; Creutzig et al., 2017). In 2020, photovoltaic power generation reached approximately 997 TWh, which constituted around 4% of the global electricity demand (IEA PVPS task 1 et al., 2021).

Solar power system (SPS) technology is characterized by its scalability, simplicity, and modularity, which contribute to lowering overall unit costs and mitigating investment risks (Wilson et al., 2020). This accessibility allows a diverse array of stakeholders globally to acquire, install, and utilize photovoltaic or solar thermal (ST) technologies. Notably, small-scale ST systems designed for the direct heating of buildings or facilities represent approximately 60% of total installations (Weiss & Spörk, 2021). In a similar vein, the photovoltaic market constitutes about 40% of distributed energy systems (IEA PVPS task 1 et al., 2021).

The considerable diversity in system sizes and applications presents challenges for stakeholders attempting to monitor historical deployments of solar thermal (ST) and photovoltaic (PV) systems, thereby complicating the assessment of global trends. The International Energy Agency Photovoltaic Power Systems Program (IEA PVPS) gathers data on the methods employed by various countries for the registration of stationary PV systems and advocates for the establishment of a compulsory database for PV systems in these nations (IEA PVPS et al., 2020). Nevertheless, in certain countries that have adopted registration databases, smaller systems may be legally connected to the grid without being officially registered, resulting in a lack of formal documentation regarding their presence (IEA PVPS et al., 2020; Stowell et al., 2020; Kasmi et al., 2022; Kausika et al., 2021). It is unrealistic to anticipate that all countries will be able to implement and maintain such a database in accordance with IEA PVPS recommendations in the foreseeable future.

A viable method for the manual documentation of fixed photovoltaic (PV) systems involves the assessment and estimation of PV system sizes through remote sensing aerial imagery obtained from satellites or aircraft, coupled with advanced deep machine learning techniques. This approach has garnered significant interest in the academic community (Ren et al., 2022). Utilizing this methodology, researchers have successfully developed databases that accurately pinpoint the locations of PV systems and categorize the types of buildings or land utilized for these installations (Kruitwagen et al., 2021; Xia et al., 2021). Furthermore, these databases can be integrated with socioeconomic data to facilitate population studies. This technique also holds promise for identifying off-grid and behind-the-meter PV systems that may be unregistered or inadequately represented to distribution system operators (DSOs) (Kausika et al., 2021). However, for effective documentation using this method, the PV systems must be observable from aerial perspectives and exhibit distinct characteristics from conventional components, which limits the detection of vertical or high-tilt systems, as well as building-integrated photovoltaics (BIPV). To date, the majority of research in this area has concentrated on the creation of training images (Bradbury et al., 2016; Kasmi et al., 2022) or the development and validation of methodologies, rather than on the generation of comprehensive statistics. Nonetheless, three notable projects have employed this approach to compile inventories of PV systems. The DeepSolar project (Wang et al., 2022) successfully identified 1.47 million PV systems across the United States using remote sensing imagery from June 2016 to September 2018, producing maps of industrial and utility-scale photovoltaic installations and generation in three global regions. The Dutch Cadastral Office reported the identification of 156,637 buildings. Additionally, Rausch et al. (2020) and Mayer et al. (2022) utilized neural network classification in conjunction with aerial imagery and 3D building data to ascertain the location, capacity, tilt, and azimuth of existing PV systems, comparing their findings with a database of 1 million buildings in the PV register.

This research seeks to advance the scientific understanding of the identification of small decentralized photovoltaic (PV) systems by employing a convolutional neural network (CNN) for aerial image classification. The study utilizes aerial imagery from a combined area across three major cities in Turkey. While similar assessments have been extensively conducted in the United States (Malof et al., 2019), the Netherlands (Kausika et al., 2021), and Germany (Rausch et al., 2020), this investigation aims to illustrate the practical application of the algorithm as both an inventory tool and a statistical method, thereby contributing to the enhancement of solar market development analyses specific to Turkey.

The Turkish photovoltaic (PV) market has traditionally been characterized by a predominantly small yet stable off-grid sector, primarily catering to holiday residences, rural homes, marine applications, and caravans. Although

Turkey lacks large-scale PV installations, the cumulative capacity of installed systems reached 8,479 MW by June 2022, accounting for 8.35% of the nation's total installed capacity (ENERJİ, 2023).

Significant advancements in agronomy, biology, informatics, agricultural robotics (Agri-robots), and artificial intelligence are driving a transformation in modern agriculture from a labor-intensive framework to a data-centric approach. Among the innovative Agri-robots, unmanned aerial vehicles (UAVs) equipped with high-resolution sensors and specialized application systems are increasingly essential for gathering multi-scale agricultural data and executing site-specific interventions. The integration of UAVs and DL is crucial for the acquisition, processing, analysis, decision-making, and implementation of agricultural information. This work begins by outlining the fundamental components of PA, UAVs, and DL, while summarizing their significant research advancements (Wang et al., 2025).

The integration of computer vision with machine learning offers a promising solution to these challenges by combining real-time observations of cloud cover with surface data collected from diverse sources. This review highlights recent advancements in solar forecasting utilizing multisensor Earth observations, emphasizing the role of deep learning, which provides a robust theoretical framework for developing architectures that can extract pertinent information from data obtained from ground-based sky cameras, satellites, weather stations, and sensor networks. In summary, while machine learning holds significant promise for enhancing the accuracy and reliability of solar energy meteorology, further research is essential to fully harness its capabilities and to address existing limitations. Ultimately, this survey aims to attract greater interest in the innovative applications of UAVs and DL in PA among multidisciplinary researchers globally, fostering further impactful and practical investigations (Paletta et al., 2023).

The innovations brought by the study to the literature:
1. Creation of a data set for aerial imagery in Turkey with software.
2. This study includes both classification and automatic segmentation of aerial images in Turkey.
3. Automatic segmentation of photovoltaic areas in aerial images with U-Net.

Figure 1 shows a block diagram summarizing the study. It can be seen from the block diagram that the study is a multi-faceted and deep study. In the first phase of the study, the dataset named OpenNRW_train_16 (Mayer et al., 2020) is used for model training. The test dataset was created by us through a long process on Google Earth. After examining the classification success of the trained models on the test dataset, we wanted to perform automatic segmentation of the test images. As can be seen in the block diagram, the images were first labeled manually with a lot of effort. Then the labeled images were automatically segmented using the U-Net model, and the success of this process was examined.

MATERIAL

For training and validation, we used the OpenNRW_train_16 open access dataset (Mayer et al., 2020), which is an upsampled dataset with a resolution of 0.05 m/pixel and contains 1,814 positive and 36,790 negative image frames from North Rhine-Westphalia, Germany.

To identify Photovoltaic Energy System installations in 3 metropolitan cities in Turkey, which is the core of our study, a test dataset was created using Google Earth (Google Earth, 2023). It took around 6 months to create the dataset from scratch. Since there are few building roof applications in city centers, the test dataset images consist of aerial images applied to rural areas and factory roofs. In the test dataset, 160 "positive" and 30,000 "negative" images were collected from the metropolitan areas of Istanbul, Ankara, and Izmir in Turkey. The images in the test dataset are scaled to 299 × 299 pixels as in the training dataset.

Figure 2 shows an example from the training dataset. It shows photovoltaic cells installed on the roof of a house. Figure 3 shows an image from the test dataset. This image was taken from Istanbul/Turkey, using Google Earth.

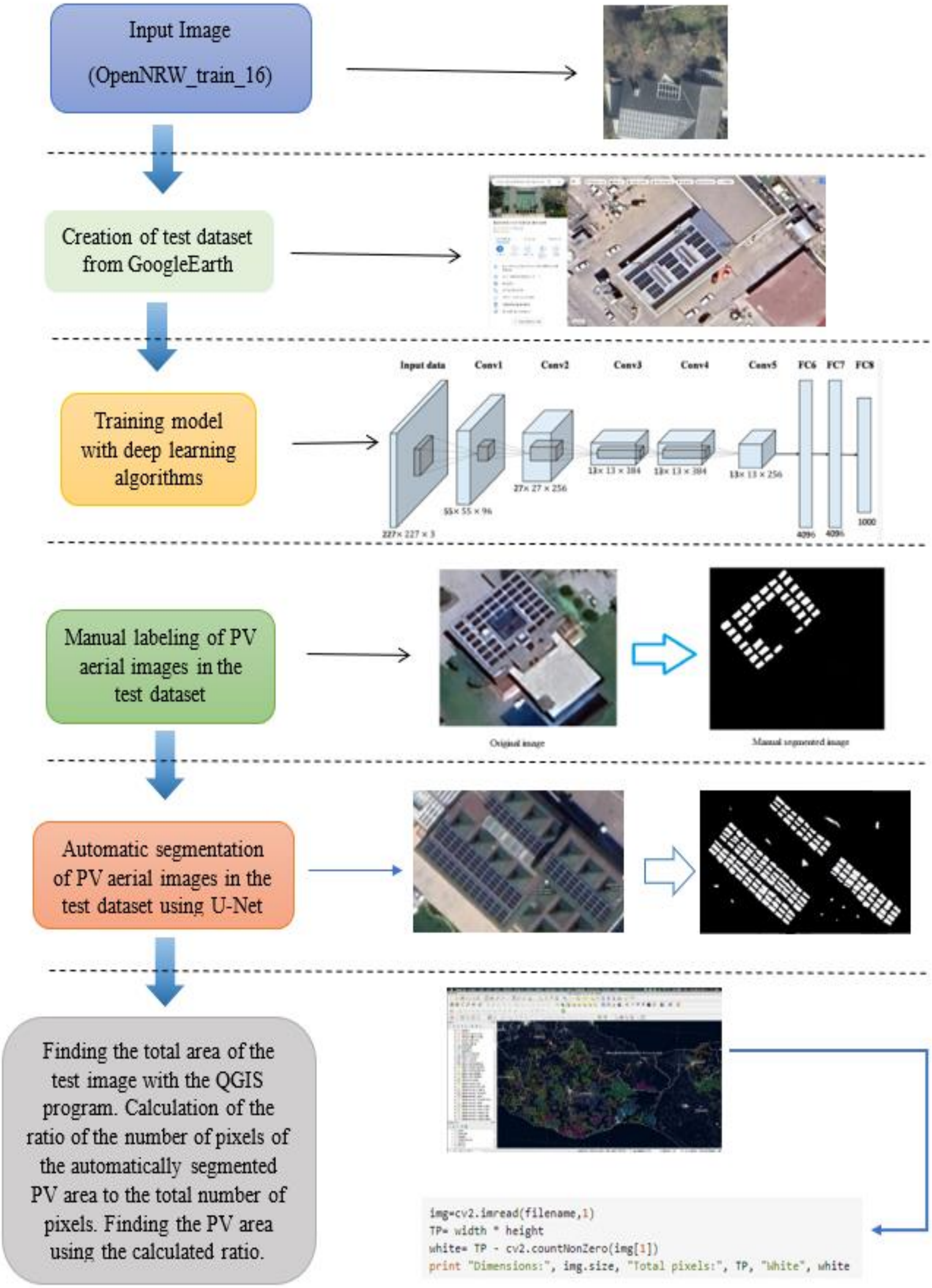

Figure 1. Processes Of The Study

Figure 2. Example From The Training Dataset

Figure 3. An Example From The Test Dataset

In the second phase of the study, images containing photovoltaic cells in the "positive" class were segmented to show the area covered by the batteries. In this phase, aerial images of photovoltaic cells in Turkey were used for training and testing. The 160 images in the "positive" class were carefully segmented manually. Figure 4 shows some examples of segmentation.

METHOD

Since there is no ready data for aerial images of photovoltaic batteries in Turkey, in the first part of the study, classification was made on image sections taken from Google Earth. The aim here is to collect aerial image sections containing photovoltaic batteries with the help of a computer by taking patches from a huge image map. Manual segmentation was performed by checking the accuracy of these images collected through computer software.

In the study, the ready dataset was trained using AlexNet, InceptionNet, and GoogLeNet models from Convolutional Neural Network (CNN) models. The classification success of these 3 trained models in the test dataset was examined (Hajabdollahi et al., 2020).

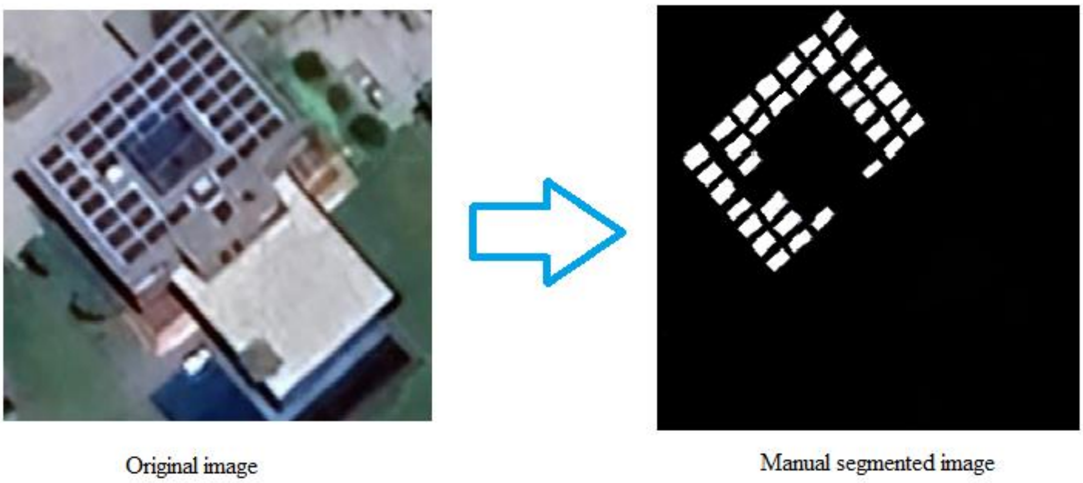

Figure 4. Segmented Image

Convolutional Neural Network

Convolutional neural networks (CNNs), often referred to as ConvNets, represent a specific category of neural networks designed for the analysis of data characterized by a grid-like structure, particularly images. Digital images serve as binary representations of visual information, comprising an array of pixels organized in a grid format. The values assigned to these pixels reflect their respective brightness and color (Garaj et al., 2021; Balcı and Alkan, 2025).

The human brain rapidly interprets a significant volume of information upon viewing an image. Each neuron operates within a specific receptive field and forms connections with other neurons to encompass the entire visual spectrum. Analogous to the functioning of neurons in a biological visual system, which respond to stimuli within a confined area known as the receptive field, neurons in a Convolutional Neural Network (CNN) similarly process data within their designated receptive fields. The architecture of these layers is structured such that basic patterns, such as lines and curves, are identified initially, while more intricate patterns, including surfaces and objects, are discerned at deeper layers. This framework enables computers to acquire visual perception capabilities.

In the forward pass, the kernel traverses the height and width of the image, generating a representation of the receptive field. This process results in a two-dimensional depiction of the image, referred to as an activation map, which illustrates the responses of the kernels at every spatial position within the image. The movement of the kernel is characterized by a parameter known as the pitch (Liu et al., 2024).

If we have an input of size W x W x D and several kernels Dout with spatial dimension F and fill amount P with S steps, the size of the output volume can be determined by the formula in Equation 1. This will give an output volume of size Wout x Wout x Dout. Figure 5 shows how the activation map is generated.

$$W_{out} = \frac{W - F + 2P}{S} + 1 \tag{1}$$

The success of the automatic classification process is visualized using the confusion matrix and ROC curve (Deng et al., 2016). Figure 6 shows how the confusion matrix is calculated.

Here; TP: Number of true positives, TN: Number of true, FP: Number of false positives, FN: False negatives.

In fact, different measures of classification success, such as accuracy, recall, and precision, are calculated from this matrix.

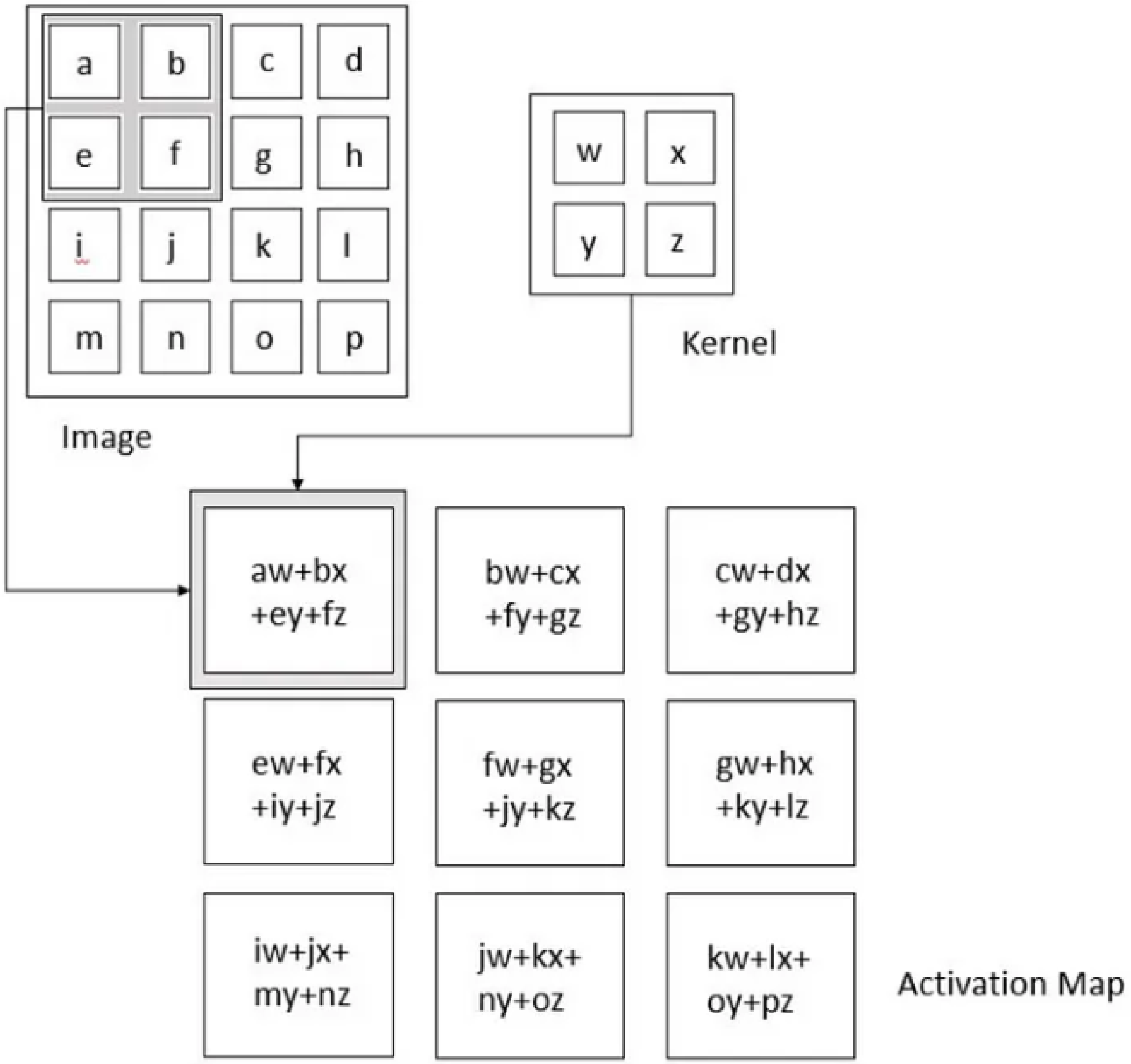

Figure 5. Convolution Process (Deep Learning, Ian Goodfellow, Yoshua Bengio, and Aaron Courville, MIT Press, 2016)

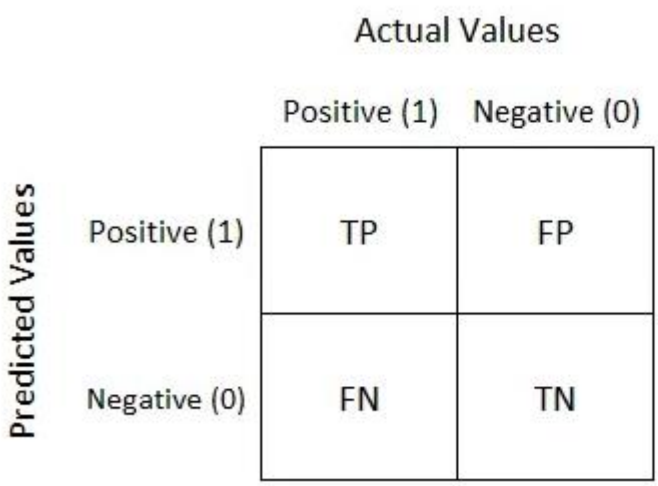

Figure 6. Confusion Matrix

Figure 7 simply shows how the ROC curve is plotted. Here, the X-axis is labeled FPR: False positive rate, and the Y-axis is TPR: True positive rate. The area under the curve gives us a numerical value between 0-1 to interpret the result. This area is called the Area of Under Curve (AUC). TPR can also be called Recall or Sensitivity and is calculated according to Equation 2. Here; TP: Number of true positives, FN: Number of false negatives.

$$TPR = \frac{TP}{TP + FN} \tag{2}$$

FPR, which forms the x-axis, is calculated according to Equation 3. Here; FP: Number of false positives, TN: Number of true negatives.

$$FPR = \frac{FP}{TN + FP} \tag{3}$$

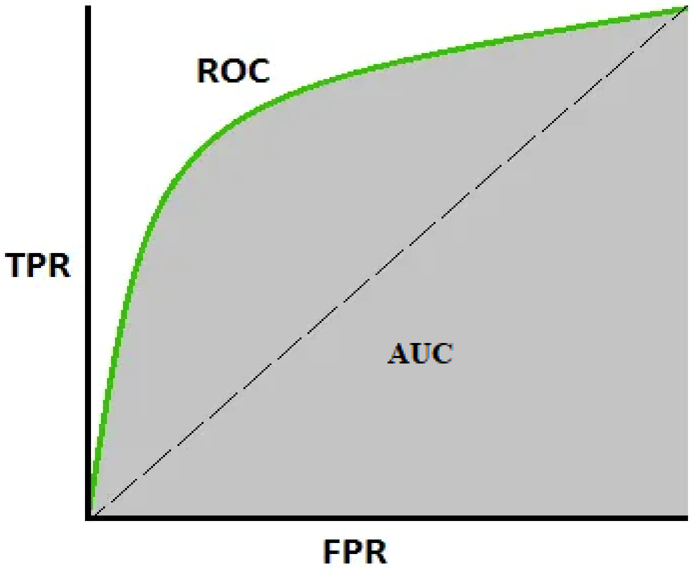

Figure 7. ROC Curve

U-Net

U-Net was initially developed for biomedical image segmentation. Its structure can be broadly categorized into a series of encoders succeeded by a series of decoders. In contrast to classification tasks, where the ultimate output of a deep learning model is of primary importance, semantic segmentation necessitates not only the ability to differentiate at the pixel level but also a method to map the distinctive features acquired at various stages of the encoder into the pixel domain. Typically, this involves utilizing a pre-trained classification network, such as VGG or ResNet, which employs convolutional layers to transform the input image into a multi-level feature representation, followed by max-pooling for subsampling. The decoder represents the latter portion of the architecture, aiming to semantically translate the features extracted by the encoder (which are of lower resolution) into the pixel space (which is of higher resolution) to facilitate dense classification. The decoder is composed of upsampling and feature fusion, followed by regularized convolution (Almalki et al., 2023; Yuan et al., 2023).

The success of image segmentation is calculated using Intersection over Union (IoU), also known as the Jaccard index. Figure 8 visualizes how the IoU score is calculated. It would be more accurate to examine Figure 8 and Equation 4 together to understand the score.

$$IoU(A, B) = \frac{(A \cap B)}{(A \cup B)} \tag{4}$$

In image segmentation, the ratio of the number of correctly predicted pixels to the number of Groundtruth pixels and the number of predicted pixels will give us the success of the segmentation with the IoU/Jaccard index.

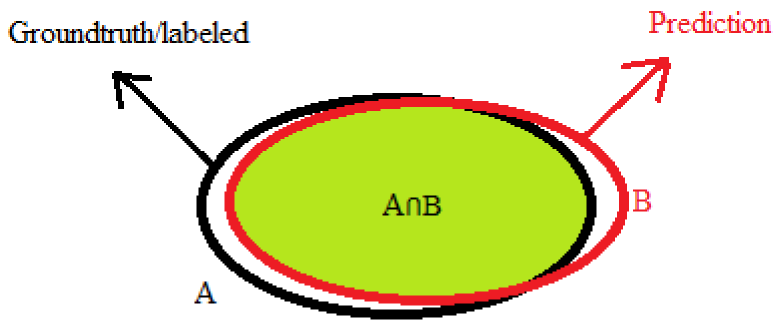

Figure 8. IoU

RESULTS

We employed the Convolutional Neural Network (CNN) deep learning approach to train our model. To enhance the performance of the CNN, we experimented with varying the number of layers within the architecture. Notable state-of-the-art CNN models include AlexNet, InceptionNet, and GoogLeNet. In the initial phase of our research, which focused on image classification, we utilized these three advanced CNN models to identify the most suitable one for our dataset. Each of the models was trained on the OpenNRW_train_16 open access dataset, comprising 1,814 positive and 36,790 negative image frames. Subsequently, the trained models were evaluated on a separate set of 160 "positive" images and 30,000 "negative" images, which had not been included in the training process and were manually sourced from Google Earth.

Three distinct deep learning algorithms were employed in this research, all of which represent cutting-edge techniques commonly referenced in existing literature. The confusion matrix serves a crucial role in the comprehensive analysis of classification outcomes. Illustrated in Figure 9 are the confusion matrices derived from the AlexNet, GoogLeNet, and Inception methodologies. Aerial images devoid of photovoltaic (PV) elements are categorized as "negative." The misclassification counts for "negatives" are recorded as 3123 for AlexNet, 3246 for GoogLeNet, and 3842 for Inception. While the misclassification figures across the three approaches are relatively close, AlexNet demonstrates the lowest incidence of "negative" misclassifications. Conversely, aerial images that include PV are designated as "positive," and Figure 9 also presents the classification results for each method. The misclassifications for the "positive" class were 17 for AlexNet, 20 for GoogLeNet, and 27 for Inception. Notably, the misclassification rates for "positives" differed from those for "negatives," with AlexNet emerging as the most effective method for the "positive" classification. Based on the confusion matrices depicted in Figure 9, it can be concluded that AlexNet is the most appropriate deep learning technique for our dataset.

Another method of interpreting the results of classification with classical and deep learning methods is the ROC curves. Figure 10 shows the ROC curves obtained with 3 different methods. In addition, AUC values showing the area under these curves were calculated and plotted. The area under the ROC curve takes a value between 0-1. The closer the classification is to 1, the more successful the classification is. However, calculating the AUC value as 1 is also undesirable due to the possibility of the method becoming rote. Figure 10 shows that the AUC value is 0.9 for AlexNet, 0.87 for GoogLeNet, and 0.83 for Inception. While AlexNet is the most successful method for classifying aerial images, Inception is the least successful of the three methods. In fact, the AUC value of 0.83 is an important classification success.

Although there are differences between the 3 methods in terms of calculating the confusion matrix and plotting the ROC curves, all 3 methods were quite successful. From this point of view, it is possible to interpret that the training and test images are suitable for processing with deep learning. Especially, the test dataset we obtained from the Google Earth application showed that it can be used in the classification process.

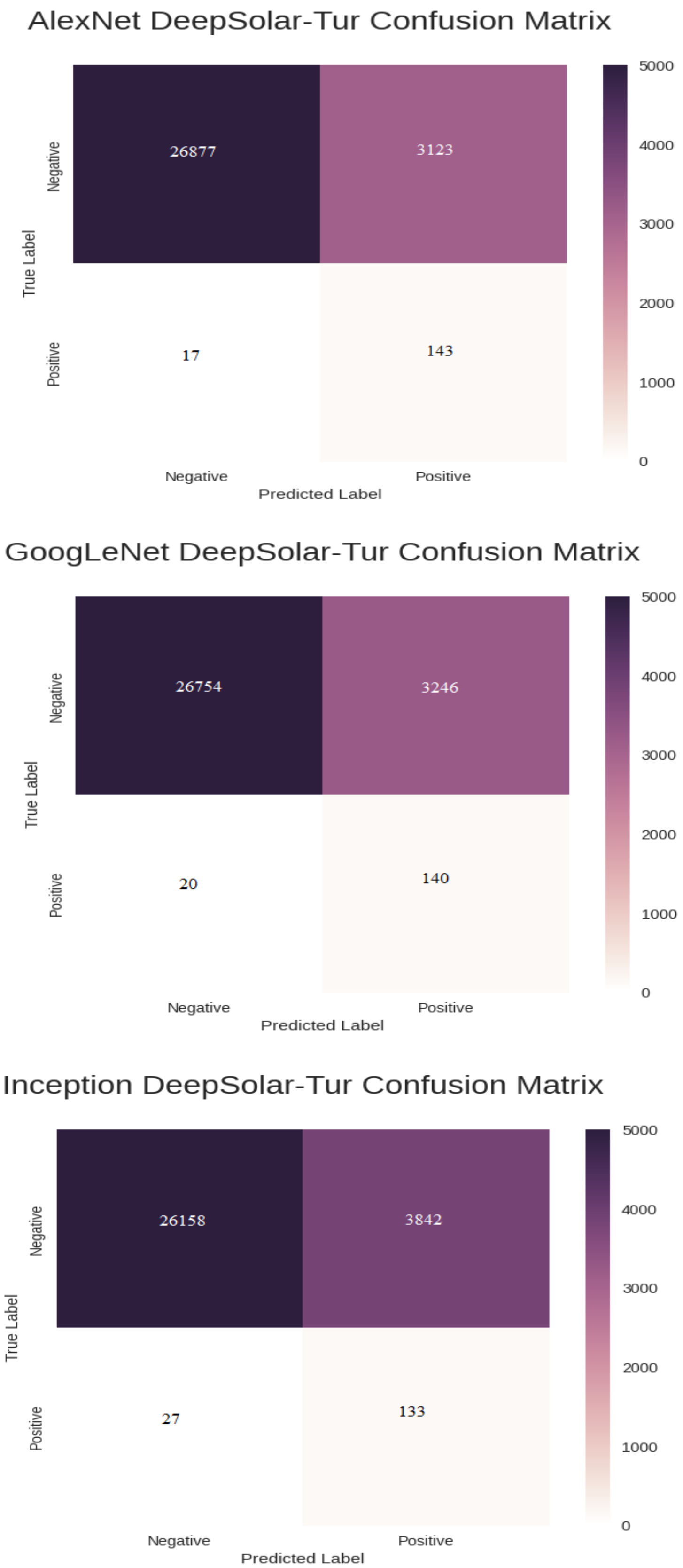

Figure 9. Confusion Matrices Of Classifications

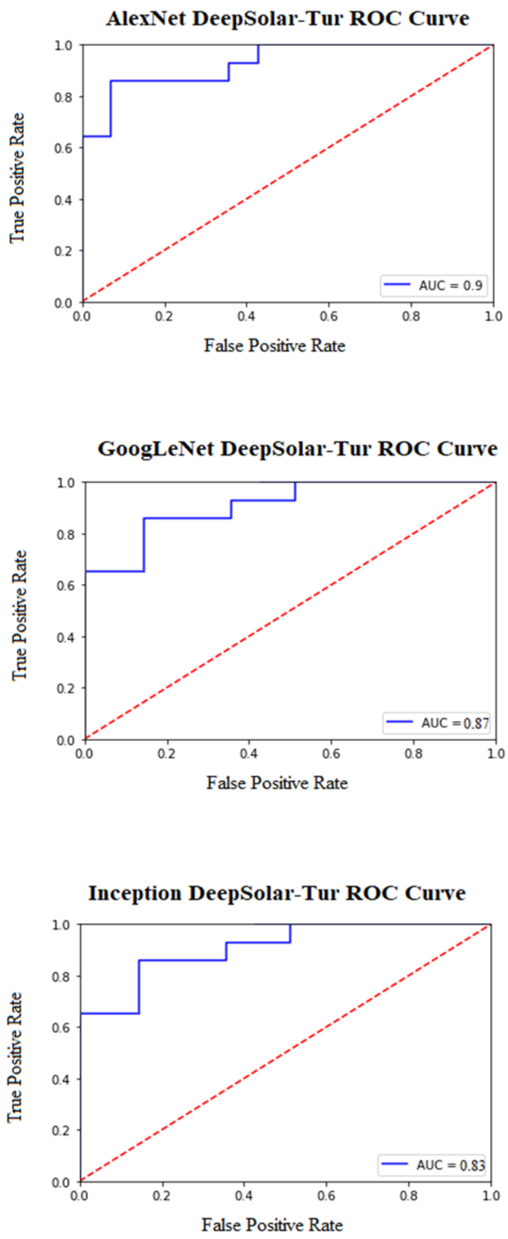

Figure 10. ROC Curves Of Classifications

U-Net segmentation is used in different disciplines and can offer high success. In our study, 2D U-Net segmentation was applied. Although the success of the segmentation is based on different scores, such as IoU, it is very important to get visual results for the application of the study. In this sense, the visual results of the segmentation obtained in our study are shown in Figure 11. As can be seen, the success of photovoltaic segmentation is also visually evident. The boundaries of the photovoltaics on the roof are clearly determined automatically. When Figure 11 is carefully analysed, the boundary of each cell is almost clear. If the clarity of the raw image in the dataset is increased, each cell in the photovoltaic system can be automatically segmented. According to our knowledge, our study is the first of its kind in Turkey. In the following stages, our study will be deepened to perform automatic segmentation at the cell level. In this way, photovoltaic applications can be planned automatically with computer software from the beginning.

Aerial images taken in different geographies may have different ambient illumination. Despite this, U-Net photovoltaic segmentation was performed at a high rate with an IoU score above 0.80, as can be seen in Figure 11. This also shows that automatic segmentation of photovoltaic areas from aerial images is possible.

Our study does not only include the classification of aerial images. Since PV detection using aerial images is the first in Turkey, to our knowledge, automatic segmentation was performed using the U-Net method at this stage of the study. We thought that visualizing the automatic segmentation would be more convenient in terms of interpreting the results, and Figure 11 shows the automatic segmentation results of some PV aerial images we randomly determined.

As can be seen in Figure 11, the automatic classifications were successful. PV locations from aerial images are clearly automatically classified. A more detailed examination of the segmentation is possible with the area calculation made at the last stage of the study. Table 1 includes the area calculation information made with manual labeling and the area calculation made with automatic segmentation. The 160 aerial images in the test dataset were obtained from Google Earth. Since the number of PVs in the images will vary, images were taken by zooming in to include all the PVs, and the size was set to 299x299 for classification. At this stage, the distance per pixel problem we encountered was solved with the QGis application (QGis, 2023). The application can be used without requiring any license. Since all 160 aerial images contain different pixel distances, pixel distance calculations were made in a study that took approximately 3 months.

Table 1 includes the PV area information obtained by manual segmentation (using QGis) and the PV area calculated by automatic segmentation (using QGis). Area information is given in square meters (m2). The total area of 7 different aerial images, manually labeled PV area, PV area calculated with automatic segmentation, and the ratio of PV areas to the whole area are given in Table 1. The ideal one for interpreting the results is the ratio of manual labeling to manual segmentation in the last row of Table 1. However, in making this interpretation, the limitation of calculating different regions as PV should not be ignored. The ratio calculation of around "1" for 7 different aerial images and the clear segmentation of PV areas in Figure 11 show that the process was successful.

CONCLUSION

The adverse consequences of fossil fuel consumption are now being experienced globally through various natural phenomena. In contemporary times, the longevity of fossil fuel resources has notably increased. In response, nations are entering into zero-emission agreements aimed at mitigating global warming and restoring the planet to its previous condition. The pervasive influence of electricity in our daily lives is indisputable, and it can be argued that the advancement of human civilization has accelerated significantly due to electricity. The advent of the internet and its electrically powered components has revolutionized access to information, allowing individuals of all ages to obtain diverse knowledge instantaneously, thereby eliminating the lengthy journeys that once characterized information retrieval. The generation of electricity, which is vital for human existence, has become increasingly critical, especially in light of the imminent threats posed by global warming. This urgency has prompted a shift towards clean energy sources for electricity production. Consequently, the concept of harnessing solar energy through photovoltaic cells has gained prominence. Initially, the first solar batteries exhibited low efficiency and incurred high installation costs. However, humanity has successfully addressed these challenges, enhancing battery efficiency and making installation more economically viable.

Countries like Turkey, situated in the solar belt, possess significant advantages regarding the availability of solar energy. Historically, individuals who harnessed solar energy for heating water have transitioned to utilizing it for electricity generation, which is essential across various sectors from production to consumption. The conversion of solar energy into electrical power holds the potential to evolve into a substantial industry. It would be reasonable to assert that nations that accurately recognize this potential and develop their infrastructure accordingly could lead the sector. Understanding the market dynamics of the photovoltaic industry is crucial for achieving market leadership. The utilization of aerial imagery can facilitate the assessment of photovoltaic cell deployment, with European nations such as Germany and the Netherlands actively engaging in research and providing support to scientists dedicated to advancing the sector. Turkey is endowed with abundant solar energy resources and has been making significant investments in solar panel manufacturing in recent years. However, there remains a gap in the creation of comprehensive data sets that could aid scientists in contributing to the industry. This study aims to address this deficiency and will serve as a valuable resource for professionals in the field.

Random selected test image-1

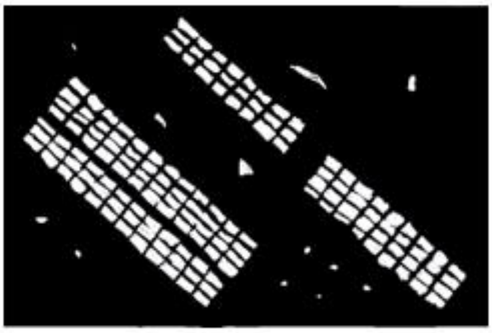

Segmented image-1

Random selected test image-2

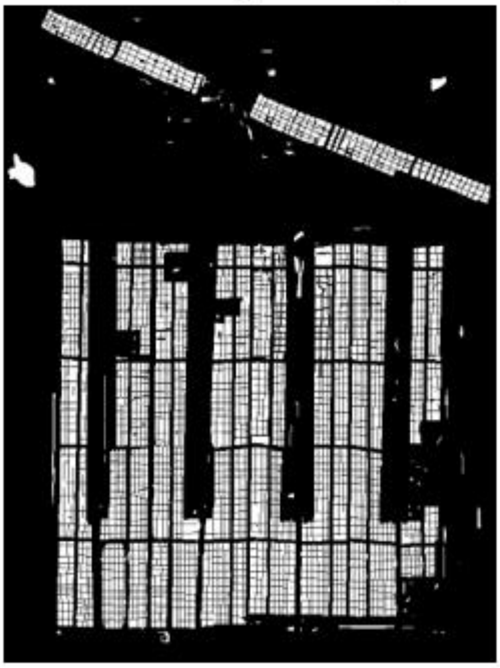

Segmented image-2

Random selected test image-3

Segmented image-3

Figure 11. Automatic Segmentation Images

Table 1. PV Area Calculations

PV aerial image number	**1**	**3**	**57**	**93**	**101**	**150**	**158**
PV aerial image total area (m2)	2561	3012	1950	2103	2480	2961	3122
Ratio of manually segmented PV area to total aerial image area	0,351	0,291	0,398	0,255	0,312	0,401	0,398
Calculated area of manually segmented PV area (m2)	898,911	876,492	776,1	513,315	773,76	1187,361	1242,556
Ratio of automatic segmented PV area to total aerial image area	0,402	0,318	0,353	0,286	0,326	0,416	0,378
Calculated area of automatic segmented PV area (m2)	1029,522	957,816	688,35	601,458	808,48	1231,776	1180,116
Ratios of manual and automatic segmentation PV by area calculation	0,873	0,915	1,127	0,853	0,957	0,964	1,053

Our study examined the subject in depth, and the test data set and manual labeling were carried out with a long study. It is a comprehensive study that tries to calculate the area of the PV-containing aerial image by automatically segmenting it from the automatic classification of the aerial image containing PV. The results obtained are quite high and reveal that more detailed studies can be carried out in the field for the Turkish example.

REFERENCES

A Garai, S Biswas, S Mandal. A theoretical justification of warping generation for dewarping using CNN. Pattern Recognit., 109 (2021), https://doi.org/10.1016/j.patcog.2020.107621.

B Rausch, K Mayer, M-L Arlt, G Gust, P Staudt, C Weinhardt, et al. An enriched automated PV registry: combining image recognition and 3D building data. ArXiv (2020).

BB Kausika, D Nijmeijer, I Reimerink, P Brouwer, V. Liem. GeoAI for detection of solar photovoltaic installations in the Netherlands. Energy AI, 6 (2021), https://doi.org/10.1016/j.egyai.2021.100111.

C Wilson, A Grubler, N Bento, S Healey, Stercke S de, C Zimm. Granular technologies to accelerate decarbonization. Science (1979), 368 (2020), pp. 36-39.

D Stowell, J Kelly, D Tanner, J Taylor, E Jones, J Geddes, et al. A harmonised, high-coverage, open dataset of solar photovoltaic installations in the UK. Sci Data, 7 (2020), pp. 1-15, https://doi.org/10.1038/s41597-020-00739-0.

D Wang, M Zhao, Z li, S Xu, X Wu, X Ma, X Liu. A survey of unmanned aerial vehicles and deep learning in precision agriculture. EUR J AGRON, 164 (2025), https://doi.org/10.1016/j.eja.2024.127477.

Deep Learning by Ian Goodfellow, Yoshua Bengio and Aaron Courville published by MIT Press, 2016.

F Creutzig, P Agoston, JC Goldschmidt, G Luderer, G Nemet, RC. Pietzcker. The underestimated potential of solar energy to mitigate climate change. Nat Energy, 2 (2017), https://doi.org/10.1038/nenergy.2017.140.

G Kasmi, L Dubus, P Blanc, Y-M. Saint-Drenan. Towards unsupervised assessment with open-source data of the accuracy of deep learning-based distributed PV mapping Workshop on Machine Learning for Earth Observation (MACLEAN), in Conjunction with the ECML/PKDD 2022 (2022). p. hal-03778289.

Google Earth , Hava görüntüleri, https:// https://earth.google.com/web (Date of acces: 16/06/2023).

IEA PVPS task 1, Masson G, Kaizuka I, Bosch E, Plaza C, Scognamiglio A, et al. Trends in photovoltaic applications — 2022. 2022.

IEA PVPS, Fechner H, Johnston W, Neubourg G, Masson G, Ahm P, et al. Data model for PV systems — Data model and data acquisition for PV registration schemes and grid connection evaluations — Best practice and recommendations. 2020.

JM Malof, B Li, B Huang, K Bradbury, A. Stretslov. Mapping solar array location, size, and capacity using deep learning and overhead imagery. ArXiv (2019), abs/1902.1.

K Bradbury, R Saboo, TL Johnson, JM Malof, A Devarajan, W Zhang, et al. Distributed solar photovoltaic array location and extent dataset for remote sensing object identification. Sci Data, 3 (2016), pp. 1-9, https://doi.org/10.1038/sdata.2016.106.

K Mayer, B Rausch, ML Arlt, G Gust, Z Wang, D Neumann, et al. 3D-PV-Locator: Large-scale detection of rooftop-mounted photovoltaic systems in 3D. Appl Energy, 310 (2022), Article 118469, https://doi.org/10.1016/j.apenergy.2021.118469.

K Mayer, Z Wang, ML Arlt, D Neumann, R. Rajagopal. DeepSolar for Germany: a deep learning framework for PV system mapping from aerial imagery. Proceedings of the 3rd International Conference on Smart Energy Systems and Technologies (SEST) (2020), pp. 11-16, https://doi.org/10.1109/SEST48500.2020.9203258.

Kasmi G, Saint-Drenan Y-M, Trebosc D, el Jolivet R, Leloux J, Sarr B, et al. A crowdsourced dataset of aerial images with annotated solar photovoltaic arrays and installation metadata, 2022, p. 1–12.

L Kruitwagen, KT Story, J Friedrich, L Byers, S Skillman, C. Hepburn. A global inventory of photovoltaic solar energy generating units. Nature, 598 (2021), pp. 604-610, https://doi.org/10.1038/s41586-021-03957-7.

L Liu , B Lin , Y Yang. Moving scene object tracking method based on deep convolutional neural network. Alex. Eng. J., 86 (2024).

M Balcı, A Alkan. Identification of wart treatment evaluation by using optimum ensemble based classification techniques. Biomed. Signal Process. Control., 95 (2024).

M Hajabdollahi, R Esfandiarpoor, E Sabeti, N Karimi, SMR Soroushmehr, S Samavi. Multiple abnormality detection for automatic medical image diagnosis using bifurcated convolutional neural network. Biomed., 57 (2020), https://doi.org/10.1016/j.bspc.2019.101792.

M Jaxa-Rozen, E. Trutnevyte. Sources of uncertainty in long-term global scenarios of solar photovoltaic technology. Nat Clim Chang, 11 (2021), pp. 266-273, https://doi.org/10.1038/s41558-021-00998-8.

M Victoria, N Haegel, IM Peters, R Sinton, A Jäger-Waldau, C del Cañizo, et al. Solar photovoltaics is ready to power a sustainable future. Joule, 5 (2021), pp. 1041-1056, https://doi.org/10.1016/j.joule.2021.03.005.

Q Paletta, G Terrén-Serrano, Y Nie, B li, J Bieker, W Zhang, L Dubus, S Dev, C Feng. Advances in solar forecasting: Computer vision with deep learning. ADV APPL ENERGY, 11 (2023), https://doi.org/10.1016/j.adapen.2023.100150.

QGis, https://qgis.org/en/site/(Date of acces: 10/06/2023).

S Ren, W Hu, K Bradbury, D Harrison-Atlas, L Malaguzzi Valeri, B Murray, et al. Automated extraction of energy systems information from remotely sensed data: a review and analysis. Appl Energy, 326 (2022), Article 119876, https://doi.org/10.1016/j.apenergy.2022.119876.

SA Almalki, S Alsubai, A Alqahtani, AA, Alenazi. Denoised encoder-based residual U-net for precise teeth image segmentation and damage prediction on panoramic radiographs. J. Dent., 137 (2023), https://doi.org/10.1016/j.jdent.2023.104651.

TEİAŞ (2019), Elektrik İstatistikleri, Aylık Elektrik İstatistikleri, https://enerji.gov.tr/eigm-yenilenebilir-enerji-kaynaklar-gunes.

W Hu, K Bradbury, JM Malof, B Li, B Huang, A Streltsov, et al. What you get is not always what you see—pitfalls in solar array assessment using overhead imagery. Appl Energy, 327 (2022), Article 120143, https://doi.org/10.1016/j.apenergy.2022.120143.

Weiss W, Spörk-Dür M. Solar heat worldwide — 2021 Edition. 2021.

X Deng, Q Liu, Y Deng, S Mahadevan. An improved method to construct basic probability assignment based on the confusion matrix for classification problem. Inf. Sci., 340-341 (2016). https://doi.org/10.1016/j.ins.2016.01.033.

Y Yuan, Z Li, W Tu, Y Zhu. Computed tomography image segmentation of irregular cerebral hemorrhage lesions based on improved U-Net. J. Radiat. Res. Appl. Sci., 16-3 (2023), https://doi.org/10.1016/j.jrras.2023.100638.

Z Wang, M-L Arlt, C Zanocco, A Majumdar, R. Rajagopal. DeepSolar++: Understanding residential solar adoption trajectories with computer vision and technology diffusion models. Joule (2022), pp. 1-15, https://doi.org/10.1016/j.joule.2022.09.011.

Z Xia, Y Li, R Chen, D Sengupta, X Guo, B Xiong, et al. Mapping the rapid development of photovoltaic power stations in northwestern China using remote sensing. Energy Rep, 8 (2022), pp. 4117-4127, https://doi.org/10.1016/j.egyr.2022.03.039.